J|A|C|S
ARTICLES

Tetrathiafulvalene Hetero Radical Cation Dimerization in a Redox-Active [2]Catenane

Cheng Wang,[†] Scott M. Dyar,[†‡] Dennis Cao,[† ±] Albert C. Fahrenbach,[†±] Noah Horwitz,[†‡]
Michael T. Colvin[†‡], Raanan Carmieli,[†‡] Charlotte L. Stern,[†] Sanjeev K. Dey, [†]
Michael R. Wasielewski[†‡]* and J. Fraser Stoddart[†±]*

[†] Department of Chemistry, Northwestern University, 2145 Sheridan Road, Evanston, IL 60208, United States

[‡] Argonne-Northwestern Solar Energy Research (ANSER) Center, Northwestern University, 2145 Sheridan Road, Evanston, IL 60208, United States

[±] NanoCentury KAIST Institute and Graduate School of EEWS (WCU), Korea Advanced Institute of Science and Technology (KAIST), 373−1 Guseong Dong, Yuseong Gu, Daejeon 305−701, Republic of Korea

SUPPORTING INFORMATION

Table of Contents

S1. X-Ray Crystallography

Data Collection for 6·4PF$_6$: A green block crystal of $C_{74}H_{84}F_{24}N_8O_8P_4S_{10}$, having the approximate dimensions of 0.45 × 0.42 × 0.17 mm, was mounted using oil (Infineum V8512) on a glass fiber. All measurements were made on a CCD area detector with graphite monochromated MoK\α radiation.

Cell constants and an orientation matrix for data collection corresponded to a monoclinic cell with dimensions: a = 22.1794(18), b = 13.6101(10), c = 29.949(2) Å, α = 90.0, β = 96.671(5) γ = 90.0º, V = 8979.4(12) Å^3.

For Z = 4 and F.W. = 2113.94, the calculated density is 1.564 g cm^{-3}. Based on a statistical analysis of intensity distribution, and the successful solution and refinement of the structure, the space group was determined to be *C*2/*c*. The data was collected at a temperature of 100 (2) K with a theta range for the data collection of 2.97 to 67.27º. Data were collected in 0.5º oscillations with 10 second exposures. The crystal-to-detector distance was 40.00 mm.

Data Reduction: Of the 32165 reflections which were collected, 7626 were unique (R_{int} = 0.0519). The linear absorption coefficient, μ(CuKα) radiation is 3.907 mm^{-1}. A numerical absorption correction was applied. Minimum and maximum transmission factors were: 0.2763 and 0.6078, respectively. The data were corrected for Lorentz and polarization effects.

Table S1. Crystal Data and Structure Refinement for **6**·4PF_6

Empirical formula	$C_{74}H_{84}F_{24}N_8O_8P_4S_{10}$
Formula weight	2113.97
Crystal size	0.45 × 0.42 × 0.17 mm
Temperature	100(2) K
Wavelength	1.54178 Å
Crystal system, space group	Monoclinic, *C2/c*
Unit cell dimensions	a = 22.1794(18) Å, α = 90.0º
	b = 13.6101(10) Å, β = 96.671(5)º
	c = 29.949(2) Å, γ = 90.0º
Volume, V	8979.4(12) $Å^3$
Z, Calculated density	4, 1.564 g cm^{-3}
Absorption coefficient	3.907 mm^{-1}
F(000)	4336
Theta range for data collection	2.97 to 67.27º
Limiting indices	$-17 \le h \le 25$, $-15 \le k \le 15$, $-34 \le l \le 34$
Reflections collected / unique	32165 / 7626 [R_{int} = 0.0519]
Completeness to Θ = 67.27	94.5%
Absorption correction	Numerical
Max. and min. transmission	0.6078 and 0.2763
Refinement method	Full-matrix least-squares on $F2$
Data / restraints / parameters	7626 / 0 / 682
Goodness-of-fit on F^2	1.058
Final R indices [$I > 2\sigma(I)$]	R_1 = 0.0848, wR_2 = 0.2275
R indices (all data)	R_1 = 0.0987, wR_2 = 0.2385
Largest diff. peak and hole	+1.515 and –0.611 e $Å^{-3}$

S2. Electron Paramagnetic Resonance Spectroscopy Characterization

EPR Measurements at X-band (9.5 GHz) were carried out at room temperature using a Bruker Elexsys E580-X EPR spectrometer outfitted with a variable Q dielectric resonator (ER-4118X-MD5-W1). All the samples were dissolved in degassed MeCN and prepared in a N_2-filled glove box to ensure the absence of oxygen. Macrocycle **1** (0.3 mM), OTTFO-TEG (0.3 mM), STTFS-TEG (0.3 mM) and **6**·4PF_6 (0.2 mM) were oxidized with varying amounts of $Fe(ClO_4)_3$. For intensity-concentration calibration curves, OTTFO-TEG and STTFS-TEG were prepared in concentrations ranging from 0.1 to 0.8 mM, each with a single equivalent of oxidant. Samples were loaded into quartz tubes (1.5 mm I.D. x 1.8 mm O.D.) and sealed with a clear ridged UV doming epoxy (Epoxies, Etc., DC-7160 UV). All the samples were used immediately after preparation. Steady-state CW EPR spectra were measured at X-band using 2 mW microwave power and 0.1 G modulation amplitude at 100 KHz, with a time constant of 5.12 ms and a conversion time of 40.96 ms.

Computational Method: The EPR spectra were simulated (Figure S2 and S3) with a home-written program in MATLAB using representative spectra of the $OTTFO^{\bullet+}$ and $STTFS^{\bullet+}$ in equal concentration measured under the aforementioned conditions. A least-squares algorithm was used to fit a linear combination of $OTTFO^{\bullet+}$ and $STTFS^{\bullet+}$ spectra to the spectra of **6**·4PF_6 after addition of varying amounts of $Fe(ClO_4)_3$. Spectral broadening was accounted for by convoluting the representative spectra with a Lorentzian function individually before fitting. The second order rate constant for spin exchange was calculated from the additional Lorentzian linewidth as determined from the fits to the experimental data. Eqns. 1 and 2, derived for the simplistic model of individual radicals diffusing in solution[S2], were used to obtain the rate constant k for spin exchange. The linewidth Γ of the Lorentzian line resulting from spin exchange broadening

is given in terms of the intrinsic linewidth Γ_0, the gyromagnetic ratio of the electron γ_e, and a lifetime between spin exchange events τ.

$$\Gamma = \Gamma_0 + |2\gamma_e\tau|^{-1} \quad (1)$$

$$k = (2\tau[R])^{-1} \quad (2)$$

Here $[R]$ is the concentration of the radical species, taken to be equal to the concentration of the catenane (0.2 mM) multiplied by the equivalents of oxidant added for samples with less than two equivalents of oxidant, and 2.00 multiplied by this concentration for samples with more than two equivalents of oxidant. The calculated rate constants for spectra showing significant broadening are on the order of 10^{10} $M^{-1}s^{-1}$, a rate that is slightly larger than those reported for nitroxide radicals in solution, which are consistent with a diffusion-controlled reaction. The large value observed in this study may be due to a similarly high rate of spin exchange, but may also reflect higher effective activities of the radicals due to their proximity in the catenane ring. Figure S4 shows the maximum signal intensity of each spectrum plotted as a function of concentration. These plots demonstrate that at low concentrations of **6**·4PF_6 (0.2 mM), the signal intensities of the representative spectra vary linearly with concentration,

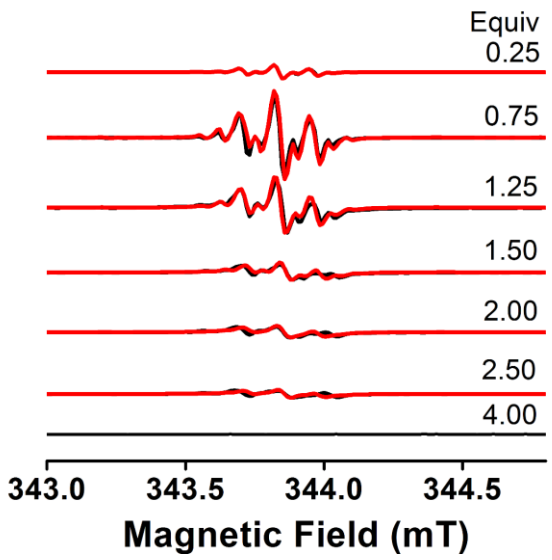

Figure S2 Simulated EPR spectra (red) overlayed on the EPR titration spectra (black) of a 2.0×10^{-4} M solution of **6**·4PF_6.

which means there is no dimerization occurring and allows us to obtain relative concentrations of oxidized species by deconvolution of the spectra.

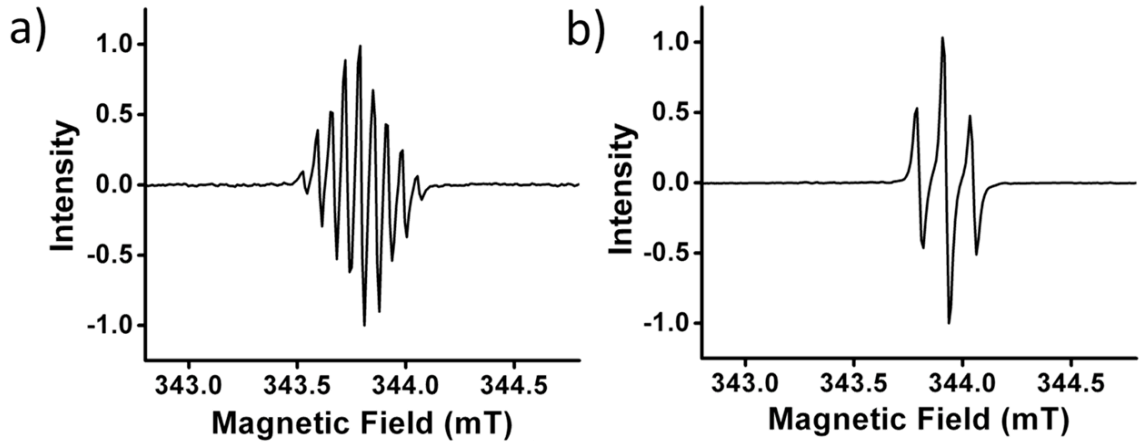

Figure S3 The $\mathbf{2}^{\bullet+}$ (a) and $\mathbf{3}^{\bullet+}$ (b) spectra used for simulations of EPR titration spectra of $\mathbf{6}\cdot 4PF_6$ after addition of oxidant. These spectra were manually aligned on the X-axis with the spectra needing deconvolution, then home-written code in Matlab was used to calculate the percent contribution of each species (Table 1 in the main text).

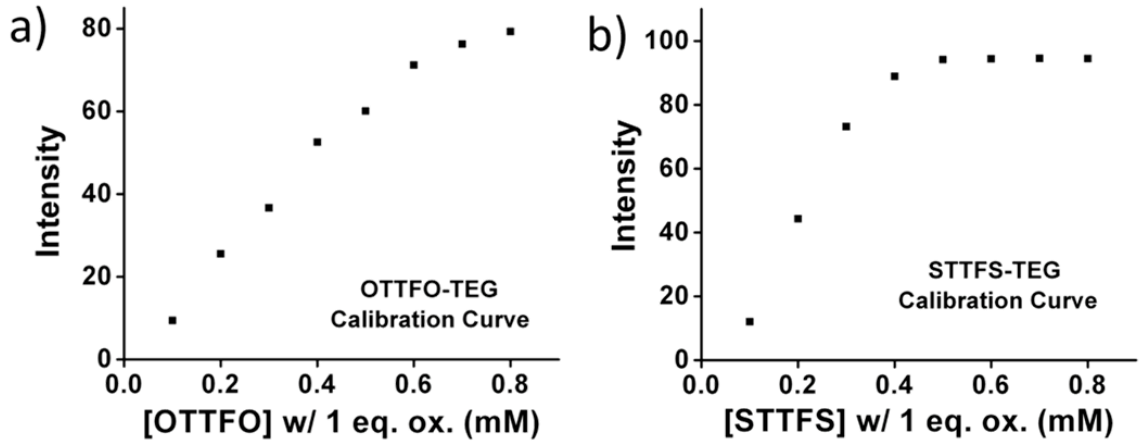

Figure S4 Titration curves of varying amounts of OTTFO-TEG (a) and STTFS-TEG (b) oxidized with 1 equivalent $Fe(ClO_4)_3$.

S3. Supplementary References

S1. Spruell, J. M.; Coskun, A.; Friedman, D. C.; Forgan, R. S.; Sarjeant, A. A.; Trabolsi, A.; Fahrenbach, A. C.; Barin, G.; Paxton, W. F.; Dey, S. K.; Olson, M. A.; Benítez, D.; Tkatchouk, E.; Colvin, M. T.; Carmielli, R.; Caldwell, S. T.; Rosair, G. M.; Hewage, S. G.; Duclairoir, F.; Seymour, J. L.; Slawin, A. M. Z.; Goddard, W. A.; Wasielewski, M. R.; Cooke, G.; Stoddart, J. F. *Nature Chem.* **2011**, *2*, 870–879.

S2. Eastman, M. P.; Kooser, R. G.; Das, M. R.; Freed, J. H. *J. Chem. Phys.* **1969**, *51*, 2690–2709.